NASA Contractor Report 178333

ICASE REPORT NO. 87-42

ICASE

COMPRESSIBLE NAVIER-STOKES EQUATIONS: A STUDY OF LEADING EDGE EFFECTS

S. I. Hariharan

P. R. Karbhari

Contract No. NAS1-18107
July 1987

INSTITUTE FOR COMPUTER APPLICATIONS IN SCIENCE AND ENGINEERING
NASA Langley Research Center, Hampton, Virginia 23665

Operated by the Universities Space Research Association

National Aeronautics and
Space Administration

Langley Research Center
Hampton, Virginia 23665

Compressible Navier-Stokes Equations: A Study of Leading Edge Effects.

S.I. Hariharan

Department of Mathematical Sciences
University of Akron, Akron, OH 44325
and
Institute for Computer Applications in Science and Engineering
NASA, Langley Research Center, Hampton, VA 23665

P.R. Karbhari

Department of Mathematical Sciences
University of Akron, Akron, OH 44325

ABSTRACT

In this study, we have developed a computational method that allows numerical calculations of the time dependent compressible Navier-Stokes equations. The current results concern a study of flow past a semi-infinite flat plate. Flow develops from given inflow conditions upstream and passes over the flat plate to leave the computational domain without reflecting at the downstream boundary. Leading edge effects are included in this paper. In addition, specification of a heated region which gets convected with the flow is considered. The time history of this convection is obtained, and it exhibits a wave phenomena.

Research for the first author was supported by a NASA contract, No. NAS1 - 18107 while he was in residence at ICASE, NASA Langley Research Center, Hampton, VA 23665, and by a grant from the National Science Foundation, Grant No. DMS - 8604047.

Compressible Navier-Stokes Equations: A Study of Leading Edge Effects.

S.I. Hariharan

Department of Mathematical Sciences
University of Akron, Akron, OH 44325
and
Institute for Computer Applications in Science and Engineering
NASA, Langley Research Center, Hampton, VA 23665

P.R. Karbhari

Department of Mathematical Sciences
University of Akron, Akron, OH 44325

1. Introduction

Computational methods applied to the Navier-Stokes equations have been a very important problem in the field of aerodynamics. The study continues due to several unanswered aspects of specific flow situations, for example, compressible flow in open domains in the presence of a plate.

The physical problem which initiated this study involved interaction of acoustic waves in the boundary layer. Such a phenomenon is important in the study of aerodynamic applications such as turboprop engine equipped aircrafts. They are known to have high fuel efficiency; unfortunately, they have high output of sound energy compared to aircrafts powered by conventional turbofan engines. Scientists working in the field wanted to understand if the noise from these turboprop engines has any favourable effects on the aircraft performance. In particular, do the sound waves interfere in a constructive sense, with the boundary layer formed during the flight? It is suspected that this phenomena is true. It is also suspected that the drag coefficient will change as the of the sound waves change. To answer this question, it is essential to have a fundamental study made available; unfortunately, there are difficulties. First these problems are hard to investigate in a mathematical sense. Secondly, it is difficult even to define acoustic sources which satisfy the field equations which are the set of perturbed compressible Navier-Stokes equations. Thus, instead of introducing acoustic sources in the flow, we propose to study generation of acoustic sources in some way, that may possibly interact with the boundary layer. Thus, we have addressed a simpler problem of a time dependent compressible fluid flow in which heating is imposed; however, no acoustic sources are introduced externally.

While these analyses appear to have been done in a sequence of papers by Rudy and Strikwerda [5,6], Bayliss, et al [2], and Abarbanel, et al [1], the results were actually constructed using a previously established boundary layer (using the code of Harris [4]) which defined the upstream or inflow boundary condition. In the current study, the flow, including the boundary layer development, is achieved by integrating the Navier-Stokes equations subject to appropriate upstream (inflow) boundary conditions. That is, the upstream values of density, temperature, and velocity components are prescribed in accordance with the physical conditions. At the downstream boundary of the computational domain, we eliminate any back flow using the nonreflective boundary condition that was developed by Rudy and Strikwerda [6]. If the flow is initialized by constant ambient values, then introducing a flat plate parallel to the flow yields the standard boundary layer solution as time increases. However, if one introduces different initial conditions in an isolated region, the flow tends to develop waves that pass through the computational domain as time increases. It is of interest to understand the nature of such waves. Our preliminary results indeed show existence of such waves. At the outset they can be thought of as acoustic waves. We plan to investigate the nature of such waves in a continuation of this study. The main purpose of this paper is to indicate the essential steps in constructing a code for this problem.

2. Mathematical Formulation

Let Ω be the infinite region in the x-y plane. Let Ω' be the region that the plate occupies (see Fig. 1). If we denote the x and y components of the velocity by $u(x,y,t)$ and $v(x,y,t)$, the pressure by $p(x,y,t)$, the density by $\rho(x,y,t)$, the total energy by $E(x,y,t)$ and the temperature by $T(x,y,t)$, then we seek to solve the initial boundary value problem to determine

$$\underline{U} = [\rho,\rho u,\rho v,E]^T \text{ in } \Omega \setminus \Omega' \text{ such that,}$$

$$\frac{\partial \underline{U}}{\partial t} + \frac{\partial \underline{F}}{\partial x} + \frac{\partial \underline{G}}{\partial y} = \underline{0} \tag{2.1}$$

where

$$\underline{F} = \begin{bmatrix} \rho u \\ \rho u^2 - \tau_{xx} \\ \rho uv - \tau_{xy} \\ Eu + Q_x - u\tau_{xx} - v\tau_{xy} \end{bmatrix}$$

$$\underline{G} = \begin{bmatrix} \rho v \\ \rho uv - \tau_{yx} \\ \rho u^2 - \tau_{yy} \\ Ev + Q_y - u\tau_{yx} - v\tau_{xy} \end{bmatrix}$$

and where the stress tensor components and heat flux are given by

$$\tau_{xx} = -p + \frac{2}{3}\mu(2\frac{\partial u}{\partial x} - \frac{\partial v}{\partial y})$$

$$\tau_{yy} = -p + \frac{2}{3}\mu(2\frac{\partial v}{\partial y} - \frac{\partial u}{\partial x})$$

$$\tau_{xy} = \mu(\frac{\partial u}{\partial y} + \frac{\partial v}{\partial x}) = \tau_{yx}$$

$$Q_x = -\kappa\frac{\partial T}{\partial x}$$

$$Q_y = -\kappa\frac{\partial T}{\partial y}.$$

The above equations are obtained when constant specific heats are assumed (calorically perfect gas). The boundary conditions are

$$u = u_\infty, \; v = 0, \text{ and } \rho = \rho_\infty \text{ as } x \to -\infty$$

$$\frac{\partial p}{\partial t} - \rho C\frac{\partial u}{\partial t} = 0 \quad \text{as } x \to \infty \tag{2.2}$$

and,

$$u = v = 0 \text{ on } \partial\Omega' \text{ (boundary of the plate).}$$

The initial conditions (at $t = 0$) are

$$u = u_\infty, \; v = 0, \; \rho = \rho_\infty, \; T = T_\infty \text{ in } \Omega.$$

Equation (2.2) specifies the nonreflective condition in an asymptotic limit. This is obtained by considering the appropriate inflow Riemann invariants for the inviscid unidirectional flow. For no reflection, the inflow variants must be zero and we obtain (2.2). This procedure is due to Hedström [8]. An improvement on this condition has been given by Rudy and Strikwerda [6]:

$$\frac{\partial p}{\partial t} - \rho C\frac{\partial u}{\partial t} + \theta(p - p_\infty) = 0. \tag{2.3}$$

Here 'θ' is a parameter that needs to be chosen optimally and works effectively even if the distance is finite. The boundary conditions (2.2) and (2.3) are in the nondimensional form; thus the governing equations (2.1) need to be cast in the same manner. This procedure is described in the Appendix A of this paper. The plan of this paper is as follows:

Beginning with the nondimensional form of the equations and boundary conditions, we shall describe the numerical procedure in the next section. This will also include the treatment of the boundary conditions numerically. Finally, the results of computations will be presented.

3. Numerical Procedure

The numerical method, commonly known as MacCormack's scheme, consists of an explicit finite difference method which is second order accurate in time and space. It is possible to increase the spatial accuracy of the method using an upgrade of the MacCormack's scheme (Gottleib and Turkel [3]); however, the viscous terms that contain the mixed derivatives in both methods are second order accurate, and thus the fourth order accuracy can be achieved only in the inviscid region. Since the accuracy in the viscous region is the most important feature, we are confined only to the second order accurate scheme globally.

For numerical computations, it is essential to truncate the infinite region Ω to one of finite size which we will denote by $\overline{\Omega}$. An obvious choice is to truncate the region as in Figure 2.

Let Γ_i be the inflow boundary, Γ_o be the outflow boundary, and let Γ_{s1} and Γ_{s2} denote the upper and lower boundaries of the calculation domain respectively. If we assign the origin at the left hand bottom corner (as in Fig. 2), then the Navier-Stokes equations (2.1) are descretized according to the explicit two stage difference formula:

$$\overline{\underline{U}}_{i,j}^{n+1} = \underline{U}_{i,j}^{n} - \frac{\Delta t}{\Delta x}\left[\underline{F}_{i+1,j}^{n} - \underline{F}_{i,j}^{n}\right] - \frac{\Delta t}{\Delta y_j}\left[\underline{G}_{i,j+1}^{n} - \underline{G}_{i,j}^{n}\right] - \Delta t \underline{H}_{i,j}^{n} \tag{3.1}$$

$$\underline{U}_{i,j}^{n+1} = \frac{1}{2}\left\{\overline{\underline{U}}_{i,j}^{n+1} + \underline{U}_{i,j}^{n} - \frac{\Delta t}{\Delta x}\left[\overline{\underline{F}}_{i,j}^{n+1} - \overline{\underline{F}}_{i-1,j}^{n+1}\right] - \frac{\Delta t}{\Delta y_{j-1}}\left[\overline{\underline{G}}_{i,j}^{n+1} - \overline{\underline{G}}_{i,j-1}^{n+1}\right] - \Delta t \overline{\underline{H}}_{i,j}^{n+1}\right\} \tag{3.2}$$

In the absence of body forces such as gravity, the nonhomogeneous terms will be zero. That is, $\underline{H} = 0$. In these formulas,

$$x_i = (i-1)\Delta x \quad \text{and} \quad y_j = \sum_{k=0}^{j-1} \Delta y_k \qquad 0 \le i \le N,\ 0 \le j \le M.$$

Thus, equations (3.1) and (3.2) require values of

$$\underline{F}_{N+1,i}\,,\ \underline{G}_{i,M+1}\,,\ \underline{F}_{0,j} \ \text{and} \ \underline{G}_{i,0}$$

which are obtained by extrapolating $\underline{F}$ and $\underline{G}$ according to the relations (3.3).

$$
\left.
\begin{aligned}
\underline{F}_{N+1,j} &= 2\,\underline{F}_{N,j} - \underline{F}_{N-1,j} \\
\underline{G}_{i,M+1} &= \frac{(\Delta y_M + \Delta y_{M-1})\underline{G}_{i,M} - \Delta y_M \underline{G}_{i,M-1}}{(\Delta y_{M-1})} \\
\underline{F}_{0,j} &= 2\,\underline{F}_{1,j} - \underline{F}_{2,j} \\
\underline{G}_{i,0} &= \frac{(\Delta y_0 + \Delta y_1)\underline{G}_{i,1} - \Delta y_0 \underline{G}_{i,2}}{(\Delta y_1)}
\end{aligned}
\right\} \qquad (3.3)
$$

It is important to note that the flux quantities $\underline{F}$ and $\underline{G}$ themselves contain derivatives with respect to x and y. Thus, the construction $\underline{F}_{i,j}$ and $\underline{G}_{i,j}$ need to be handled in a special way and they are given in Table 1. This is the same procedure given by Anderson, et al [9].

$\left[\frac{\partial f}{\partial x}\right]_{i,j} =$			
	$\underline{F}$	Predictor	$\frac{f_{i,j} - f_{i-1,j}}{\Delta x}$
		Corrector	$\frac{f_{i+1,j} - f_{i,j}}{\Delta x}$
	$\underline{G}$	Predictor	$\frac{f_{i+1,j} - f_{i-1,j}}{2\,\Delta x}$
		Corrector	$\frac{f_{i+1,j} - f_{i-1,j}}{2\,\Delta x}$

Table 1. x - derivatives where 'f' denotes 'u,' 'v,' or 'T'

The y derivatives are handled globally as follows:

$$
\left[\frac{\partial f}{\partial y}\right]_{i,j} = \begin{cases} \dfrac{f_{i,j+1} - f_{i,j}}{\Delta y_j} & \text{.....above the plate,} \\ \dfrac{f_{i,j} - f_{i,j-1}}{\Delta y_{j-1}} & \text{.....below the plate.} \end{cases}
$$

The two differencing formulas in the y direction were motivated by the boundary conditions on the plate, which is discussed later. However, the accuracy is possibly decreased, and it requires further investigation.

The above discussion completes the finite difference relations inside the computational domain. We also require the differencing relation on the physical and nonreflective boundary conditions mentioned in section 2.

4. Discrete Form of the Boundary Conditions

Recall on the inflow boundary Γ_i, that ρ, u, and v were specified. In addition we specify T at the inflow. While this may be an over specification, this is one of the choices to make the initial value problem well-posed. Details are seen in [6]. This translates into

$$\left.\begin{aligned} \rho_{1,j} &= \rho_\infty \\ T_{1,j} &= T_\infty \\ u_{1,j} &= u_\infty \\ v_{1,j} &= 0 \end{aligned}\right\}_{(1 \le j \le M)} \tag{4.1}$$

In the set of equations (4.1), the quantities with subscripts ∞ denote the upstream values and are given in Appendix B. On the boundaries Γ_{s1} and Γ_{s2}, the condition $v = 0$ is imposed to indicate the inviscid nature of the flow away from the plate. This, when written in discrete form, is

$$v_{i,j} = 0 \qquad (1 \le i \le N) \quad (j = 1 \text{ or } M). \tag{4.2}$$

The outflow conditions are the same as that used by Rudy and Strikwerda [6]. In their work they show a set of four outflow boundary conditions against computational efficiency. In this work, the choice was the set which is mathematically most consistent but a bit slower in achieving convergence. Here we calculate the pressure from the discrete form of the nonreflective condition (2.3) and then calculate temperature using the equation of state for a gas which is calorically perfect (constant specific heats):

$$p = (\gamma - 1)\rho T \tag{4.3}$$

The discrete form of the nonreflective condition (2.3) is

$$p_{N,j}^{n+1} = \frac{1}{(1 + \theta\Delta t)} \left[p_{N,j}^{n} + \theta\Delta t p_\infty^n + \rho_{N,j}^n C_{N,j}^n (u_{N,j}^{n+1} - u_{N,j}^n) \right] . \tag{4.4}$$

Using relation (4.3), the temperature is determined by

$$T_{N,j}^{n+1} = \frac{p_{N,j}^{n+1}}{(\gamma - 1)\rho_{N,j}^{n+1}}. \tag{4.5}$$

The speed of sound, C, is calculated according to (See Appendix A)

$$C_{i,j} = \sqrt{\gamma(\gamma - 1)T_{i,j}}. \tag{4.6}$$

Finally u,v and ρ are prescribed by zeroth order extrapolation on the outflow boundary.

Along the plate, both u and v are zero and the temperature of the plate is maintained at T_∞ . In addition it is necessary to impose $\frac{\partial p}{\partial y} = 0$ (see [6]). The discrete forms of these conditions are

$$\left.\begin{aligned} T_{i,jP} &= T_\infty = T_{i,jP-1} \\ u_{i,jP} &= 0 = u_{i,jP-1} \\ v_{i,jP} &= 0 = v_{i,jP-1} \\ p_{i,jP+1} &= p_{i,jP} \\ p_{i,jP-2} &= p_{i,jP-1} \end{aligned}\right\} \qquad (4.7)$$

where jP indicates the upper boundary of the plate and jP-1 is the lower one.

The differencing used for y derivatives in the viscous terms is different than that suggested by Anderson, et al [9]. The reason we give for this change is as follows: the backward difference at jP or the forward difference at jP-1 yields $\partial u/\partial y = 0$ which is not consistent with existing physical conditions on the plate (in fact, $\partial u/\partial y = 0$ implies no velocity gradients at the plate which means inviscid flow!). To overcome this difficulty, we have used forward differencing in the y region above the plate and backward differencing in the region below. In addition to boundary conditions, initial conditions and reference values must be specified .

5. Numerical Results and Discussions

With the numerical scheme described in the last section, a code was developed. Calculation was started from a state of rest with initial conditions ρ_∞, u_∞, v_∞, and T_∞ . The solution was monitored for a change in solution of the order of 10^{-6} in each dependent variable in the successive calculations. If ϕ is any of the dependent variables, then convergence was assumed when

$$\max_{\Omega} \left| \phi_{i,j}^{n} - \phi_{i,j}^{N+1} \right| = \leq 10^{-6}.$$

To achieve this convergence, typically 60,000 steps were needed. It is also important to note that the Reynold's number used in the calculation is 1.5×10^5 for the configuration considered with $L_{ref} = 1$ ft.

At this point we remark that the time step Δt was chosen well below the stability limit that was prescribed by MacCormack [9]. A nondimensional time step of 10^{-5} was chosen for the calculations for the meanflow and for the case in which there were no thermal disturbances. Moreover, to capture as many points as possible inside the boundary layer while keeping the upper boundary of the calculation domain as far away from the plate as possible, stretching was used. The stretching was obtained using the following formula,

$$\bar{y} = 1 - \frac{1}{\lambda} \ln \left[\frac{\beta + 1 - y}{\beta - 1 + y} \right] \quad . \qquad (5.1)$$

This stretching was above the plate and was reflected in the plate to get a symmetric grid. The plate was assumed to have a thickness of a mesh layer adjacent to it. The value of β used was 1.000001. Such a transformation is due to Roberts [10]. The total number of grid points in the x direction was 60 and also 60 in the y direction.

The first case here is to let the flow develop the boundary layer. Mach number for all cases considered here was 0.4. The mesh thickness in the x direction was 0.3, and the computational domain has an aspect ratio of roughly .95. The tuning parameter at the outflow boundary condition θ was chosen to be 1.1 and was found to be optimal by experimentation. Plate is assumed to have a mesh width in the y direction and is thin due to the stretching. The leading edge of the plate is located at the 9th grid point in the x direction. Prandtl number was 0.72. Uniform initial conditions were used in the entire computational domain and the algorithm was initiated to reach a convergence of the order 10^{-6} in 60,000 time steps. The result was compared against the incompressible case Blasius's solution and is given in Figure 3. The comparison was made at the 25th x- grid point on the plate. We obtained 9 points in the boundary layer. Numerical values are given in Table 2.

Since these computations contain the leading edge, and very little is known about this situation in the computational literature, it is interesting to see the flow field at the last step of the calculation. We chose to present the flow field in the entire computational domain. In Figure 4 we see the u velocity component. The valley of the graph is the boundary layer region. The flow is moving from left to right. The flanged level indictes the region where the value of u has reached 1, the uniform flow condition. At the leading edge, we see some disturbances as expected. At the trailing edge where we had imposed the nonreflective condition, we see some reflections, because the boundary condition is not completely nonreflective. This could be improved by a more accurate nonreflective condition, about which unfortunately very little is known in the literature. Alternatively, it could be improved by stretching the computational domain at farther distances which will increase the computational time substantially. Settling for the current results that we have, we took a closer look at the flow, particularly at the leading edge. We opted to look at the crossection through a contour plot, which is shown in Figure 5. Stagnation region is clearly seen from the figure, and the flow tends to spread at the leading edge. An even more interesting feature that we observed is that of the v (y - velocity) component. This is shown in Figure 6. As we see above and below the plate, the velocity seems to undergo a cycle in opposite directions at the leading edge. A reverse cycle seems to take place at the trailing edge. It suggests that a vorticity pattern is created at the leading edge and the trailing edge, where the nonreflective condition is imposed. Taking a closer look at the crossection through the contours, in Figure 7, we see periodic orbits corresponding to the disturbances at the leading edge. They also exist at the trailing edge, but exhibit inaccuracies in the nonreflective boundary condition. Such phenomena need further investigation, and we are unable to explain it fully in this paper.

To investigate the wave phenomena, we initialized a temperature which has a value twice that of the ambient value in a small region of 4 mesh size just above the leading edge. As the flow moves the temperature certainly gets convected along the flow and finally reaches a steady value. But in this transition we suspect that the nature of convection should be of a wave phenomenon, in partcular an acoustic one. To understand this transition, we plotted the time history of the temperature, which we saved at every step of integration. However, it is known that the numerical scheme itself has its own nature of oscillations. To separate this effect, we plotted the time history of the temperature in the same region without initializing higher temperature. This is shown in Figure 8. We then computed the time history of the heated region, which is shown in Figure 9. It is clear that the time history in the heated region has a different frequency of oscillations than the one with no heat, exhibiting a true wave phenomenon. Finally we compared the case of the heated region and the case unheated region in the same graph (Figure 10). Clearly we see the oscillations that correspond to the numerical scheme and the ones that correspond to the physical situation. In particular, up to the value of time t = .1 , we see a high frequency oscillation. It should be noted that similar concepts are found in reference [7], where a simple driven cavity problem was considered for these purposes.

It is curious to know what happens to the boundary layer in the presence of the heated region. After 60,000 time steps for each case (with and without heated region) we constructed the values of u - velocity component within the boundary layer as before. Although the numerical values do not differ by a substantial amount; there are differences. The results are given below.

TABLE 2

Boundary Layer Solutions at i = 25		
Point	Regular Flow	Flow with Heat
0	0.00000	0.00000
1	0.23222	0.23221
2	0.45365	0.45372
3	0.65929	0.65933
4	0.81739	0.81739
5	0.92020	0.92023
6	0.97135	0.97131
7	0.99170	0.99168
8	0.99801	0.99799

* (0 represents the plate level)

All our computations were performed on a SUN Microsystem (3/260) with a floating point accelerator. Double precision calculations took 65 CPU hours of computation in each case.

From our computations, it is clear that two important things need to be investigated in the future. First, the leading edge singularity needs to be understood further by computational work with a theoretical backing. Second is of course, the nature of these waves; again to isolate the nature, theoretical ideas are needed. While there is a large amount of literature available to interpret these phenomena for incompressible flows, we are not aware of satisfactory theoretical work to explain these results for the compressible flow situation. We intend to continue this work in the future to answer these questions.

Appendix A

Nondimensionalization

Let L be a characteristic length in the flow domain. Our coordinate distances x and y are nondimensionalized with respect to this length. We also define reference values for which all of the thermodynamic and fluid quantities are known. These are denoted by the subscript "ref." We note that these reference values and the conditions at negative infinity may very well be the same (but not necessarily). With this, we can write

$$\bar{x} = x/L \qquad \bar{y} = y/L \qquad \bar{t} = \frac{t}{L/u_{ref}}$$

$$\bar{u} = u/u_{ref}, \qquad \bar{v} = v/v_{ref}$$

$$\bar{\mu} = \mu/\mu_{ref}, \qquad \bar{\rho} = \rho/\rho_{ref}, \qquad \bar{p} = p/p_{ref}$$

$$\bar{T} = T/T_{ref}, \qquad \bar{e} = e/e_{ref}, \qquad \bar{E} = E/E_{ref}.$$

Some of the above quantities are not independent. The relationships are as follows:

$$e_{ref} = u_{ref}^2$$

$$p_{ref} = \rho_{ref} u_{ref}^2$$

$$E_{ref} = \rho_{ref} e_{ref} = \rho_{ref} u_{ref}^2 .$$

The equation of state, when subjected to the above nondimensionalization, gets converted as follows:

$$p = \rho R T$$

$$\bar{p} = \left[\frac{\rho_{ref} R T_{ref}}{p_{ref}}\right] \bar{\rho} \bar{T}.$$

Dropping the bar notation for convenience,

$$p = \beta \rho T \qquad \text{where, } \beta = \frac{\rho_{ref} R T_{ref}}{p_{ref}} = \frac{R T_{ref}}{u_{ref}^2}.$$

Now,

$$T_{ref} = \frac{u_\infty^2}{c_v} \quad \text{and} \quad u_{ref} = u_\infty$$

(Note that we have equated the reference plane and infinity) which yields

$$\beta = (\gamma - 1)$$

and

$$p = (\gamma - 1)\rho T.$$

The Navier-Stokes equation takes the following nondimensional form:

$$\frac{\partial \underline{U}}{\partial t} + \frac{\partial \underline{F}}{\partial x} + \frac{\partial \underline{G}}{\partial y} = \underline{0} \tag{2.1}$$

where

$$\underline{U} = \begin{bmatrix} \rho \\ \rho u \\ \rho v \\ E \end{bmatrix}$$

$$\underline{F} = \begin{bmatrix} \rho u \\ \rho u^2 - \tau_{xx} \\ \rho uv - \tau_{xy} \\ Eu - \mu_\alpha \dfrac{\partial T}{\partial x} - u\tau_{xx} - v\tau_{xy} \end{bmatrix}$$

$$\underline{G} = \begin{bmatrix} \rho v \\ \rho uv - \tau_{yx} \\ \rho v^2 - \tau_{yy} \\ Ev - \mu_\alpha \dfrac{\partial T}{\partial y} - u\tau_{yx} - v\tau_{xy} \end{bmatrix}$$

and where the stress tensor components and energy are given by

$$E = \rho\left[e + \frac{u^2 + v^2}{2}\right]$$

$$\tau_{xx} = -p + \frac{2}{3}\frac{\mu}{Re}\left(2\frac{\partial u}{\partial x} - \frac{\partial v}{\partial y}\right)$$

$$\tau_{yy} = -p + \frac{2}{3}\frac{\mu}{Re}\left(2\frac{\partial v}{\partial y} - \frac{\partial u}{\partial x}\right)$$

$$\tau_{xy} = \frac{\mu}{Re}\left(\frac{\partial u}{\partial y} + \frac{\partial v}{\partial x}\right) = \tau_{yx}$$

and

$$\mu_\alpha = \frac{c_p T_{ref}}{Pr\, Re\, u_{ref}^2} \qquad Re = \frac{\rho_{ref} u_{ref} L}{\mu_{ref}} \quad , \quad Pr = \frac{c_p \mu_{ref}}{k_{ref}}.$$

In these calculations, we have used $\mu\alpha = \bar{\mu}$.

To calculate the speed of sound, 'C,'

$$C = \left[\frac{\gamma p}{\rho}\right]^{1/2}$$

$$= \left[\frac{\gamma(\gamma - 1)\rho T}{\rho}\right]^{1/2} \qquad \text{since } p = (\gamma - 1)\rho T$$

$$= \sqrt{\gamma(\gamma - 1)T}.$$

Aknowledgement

The authors wish to thank Dr. Bruce B. Henriksen of Department of the Army, Redstone Arsenel, for his input in the concept of producing acoustic waves in the heated region. Authors are also grateful to Mr. Ronald L. Gaug of University of Akron for his outstanding help with our SUN computer environment.

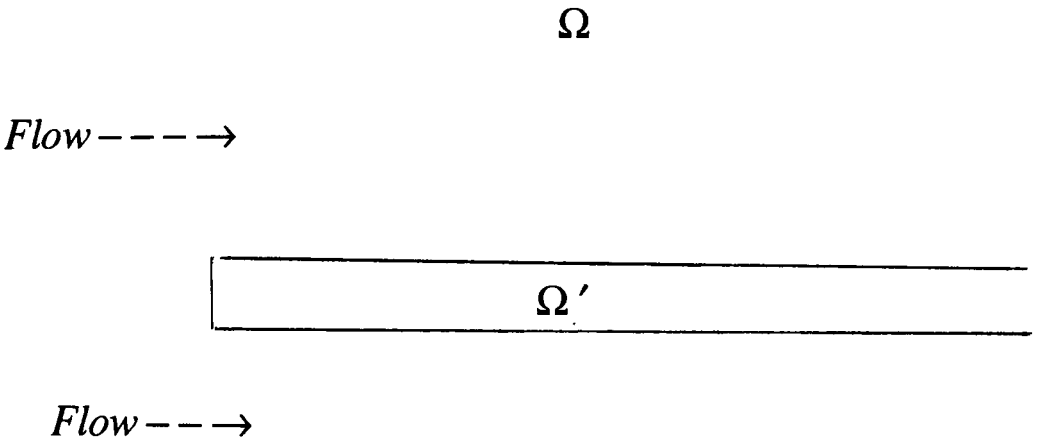

Figure 1

PHYSICAL FLOW FIELD DOMAIN

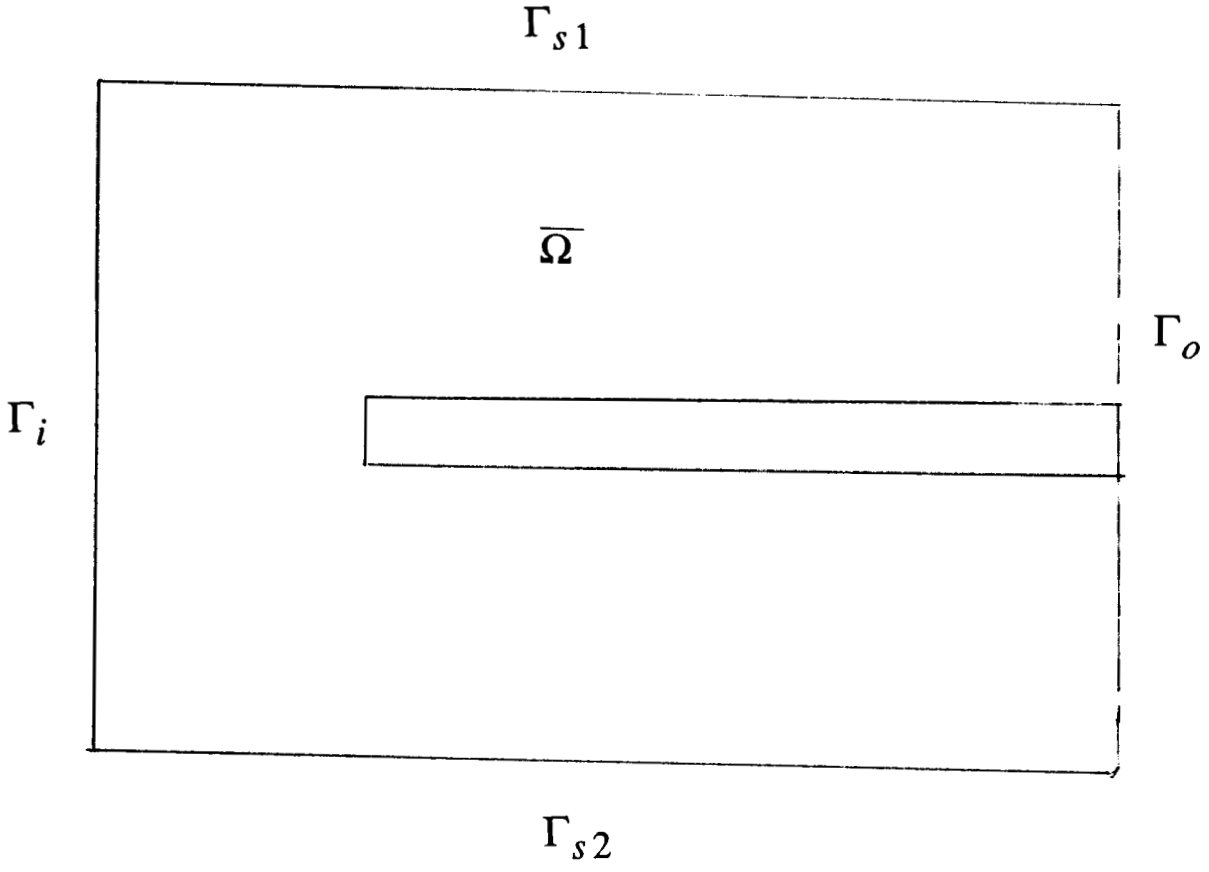

Figure 2

COMPUTATIONAL FLOW FIELD DOMAIN

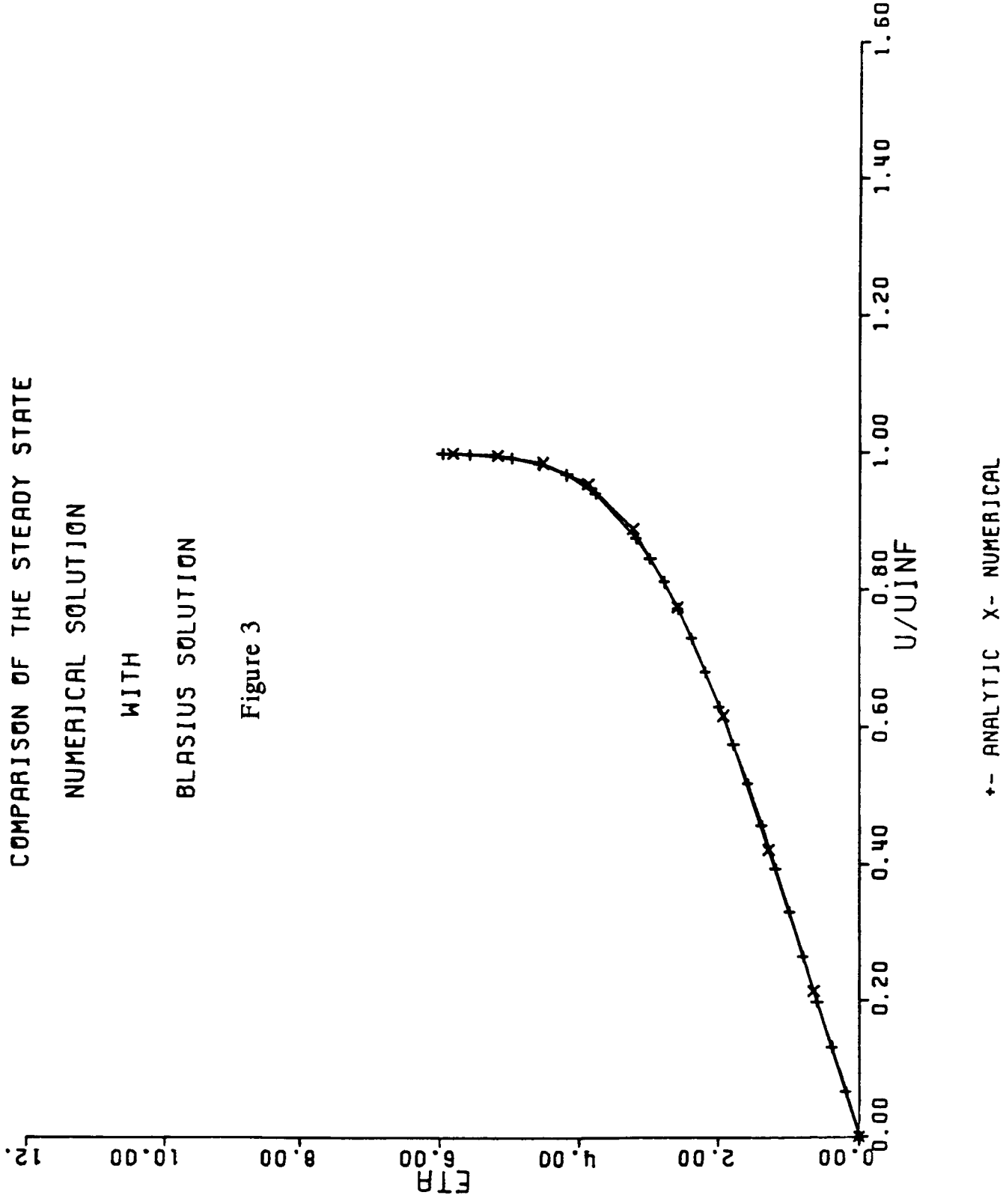
COMPARISON OF THE STEADY STATE
NUMERICAL SOLUTION
WITH
BLASIUS SOLUTION
ETA
0.00
2.00
4.00
6.00
8.00
10.00
12.
0.00
0.20
0.40
0.60
0.80
1.00
1.20
1.40
1.60
U/UINF
+- ANALYTIC X- NUMERICAL

Figure 3

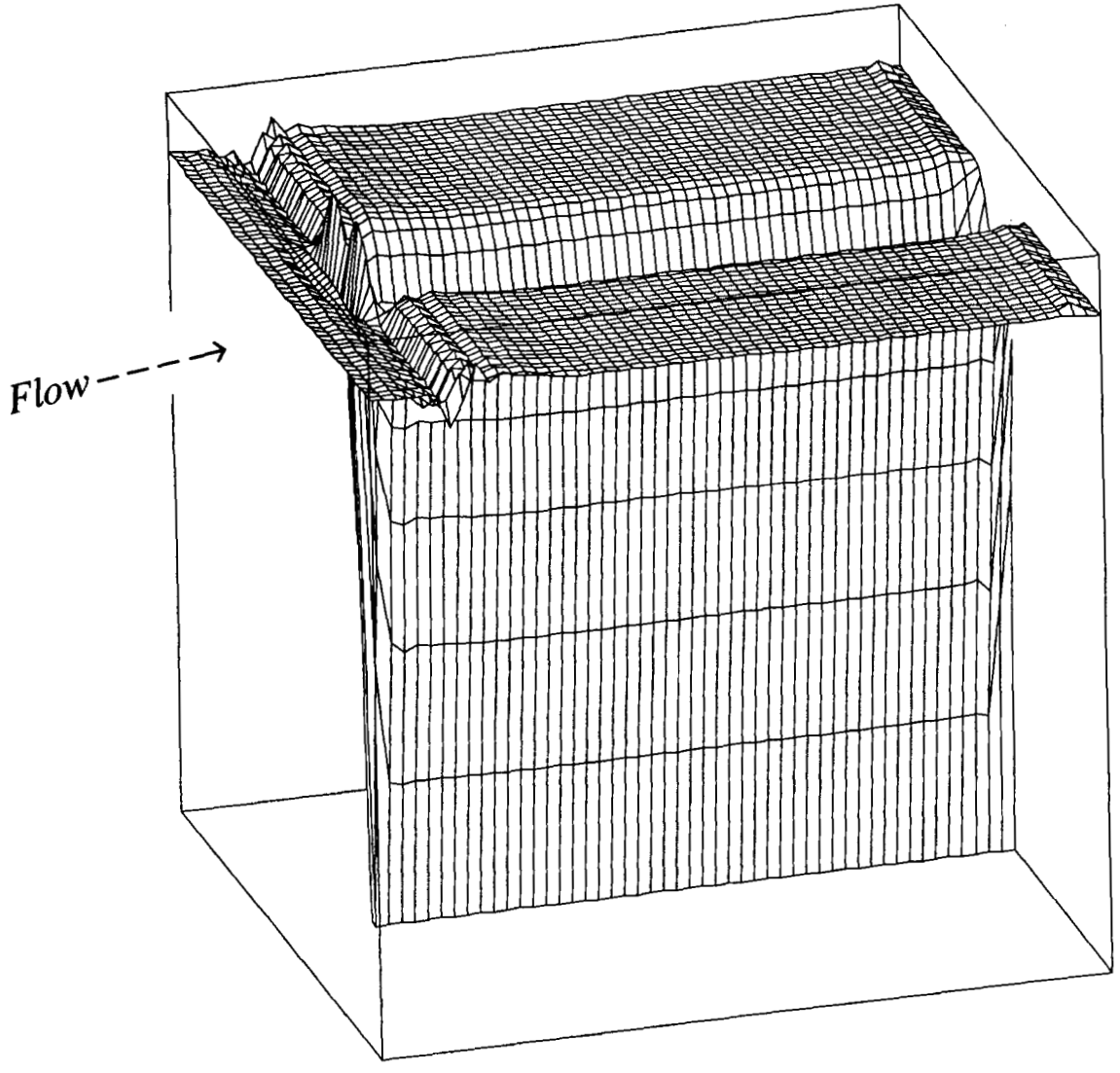

Figure 4 u - velocity z = u(x,y)

Figure 5

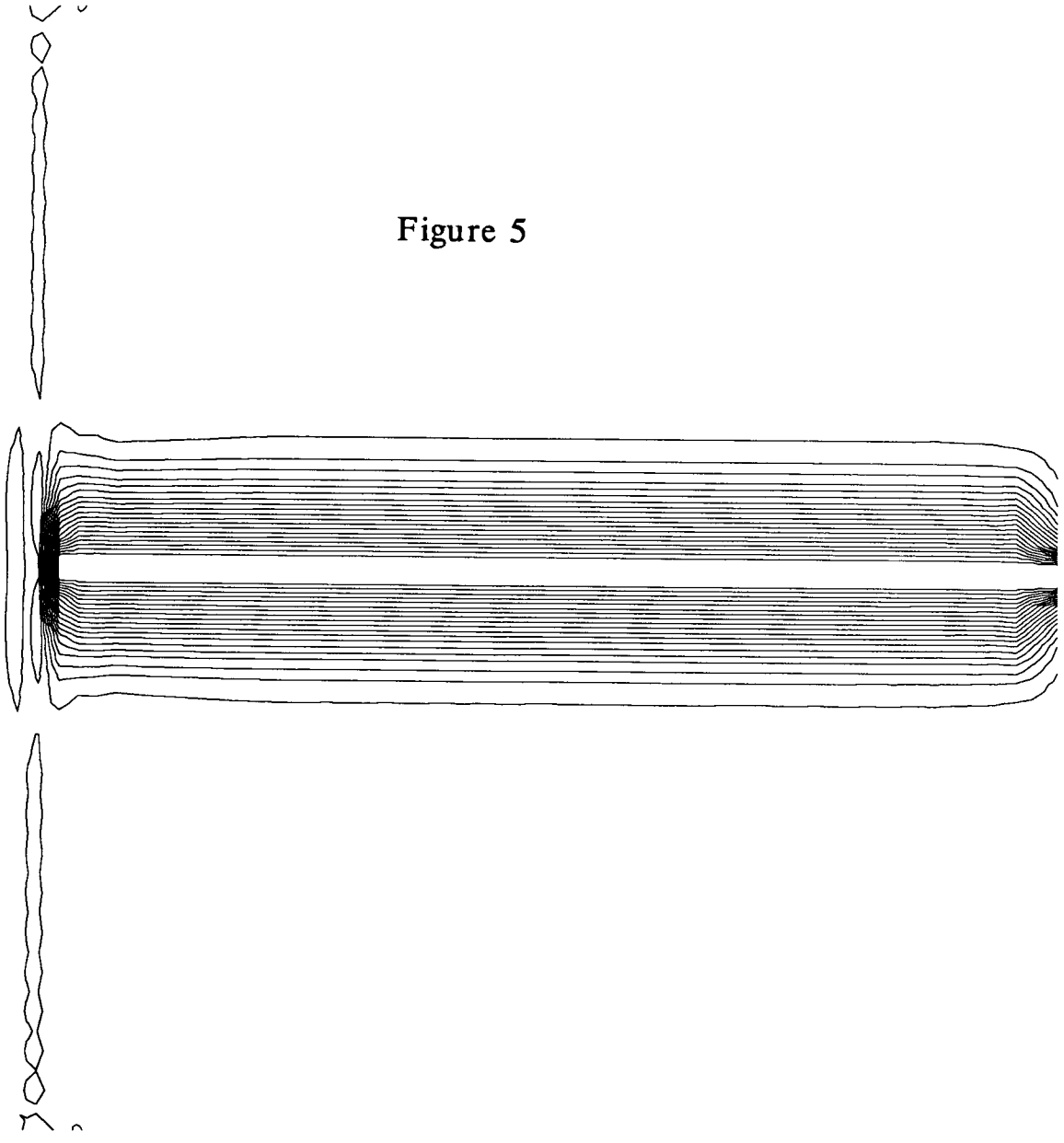

u Velocity Contour

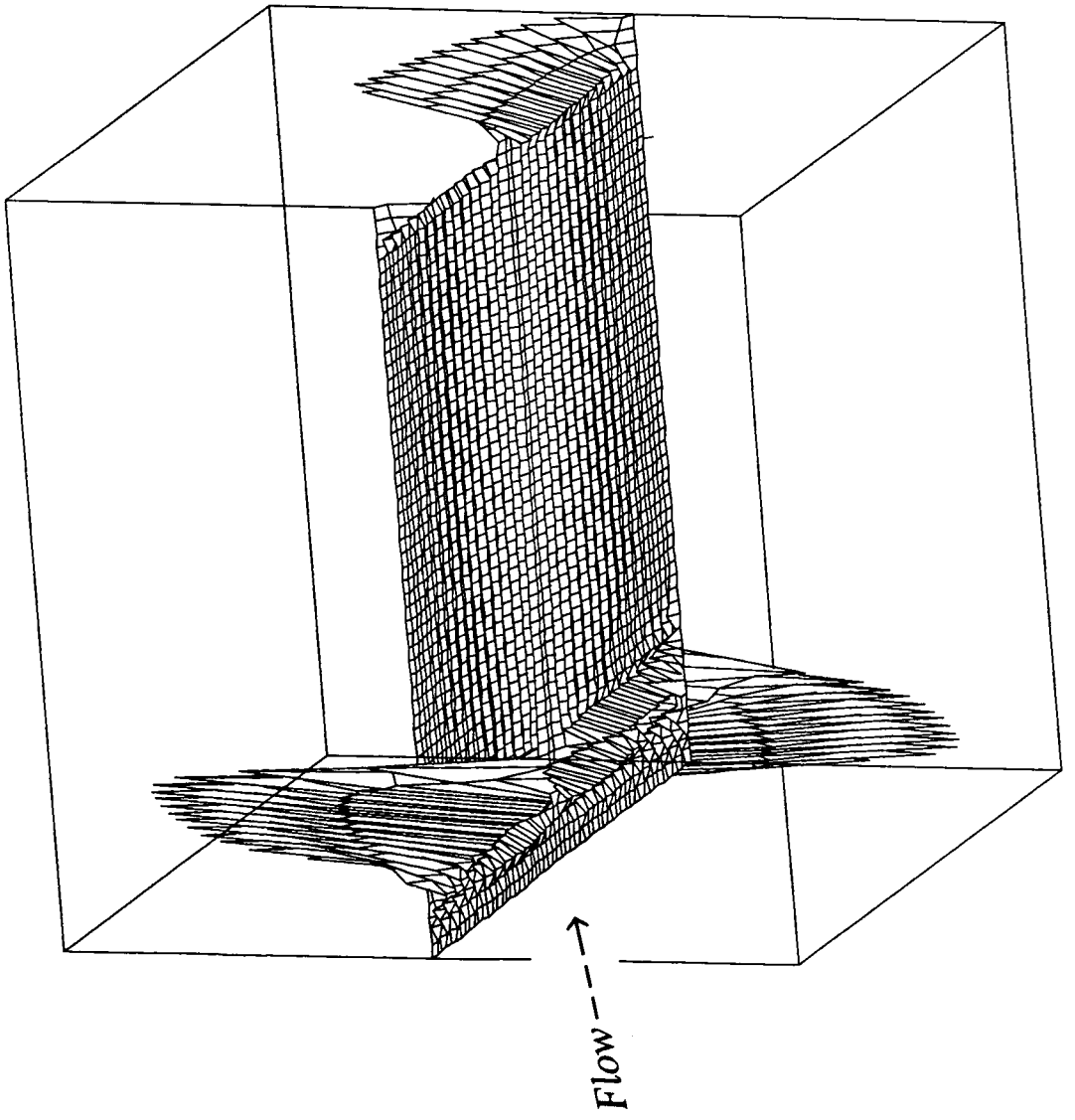

Figure 6 v - velocity z = v(x,y)

Figure 7

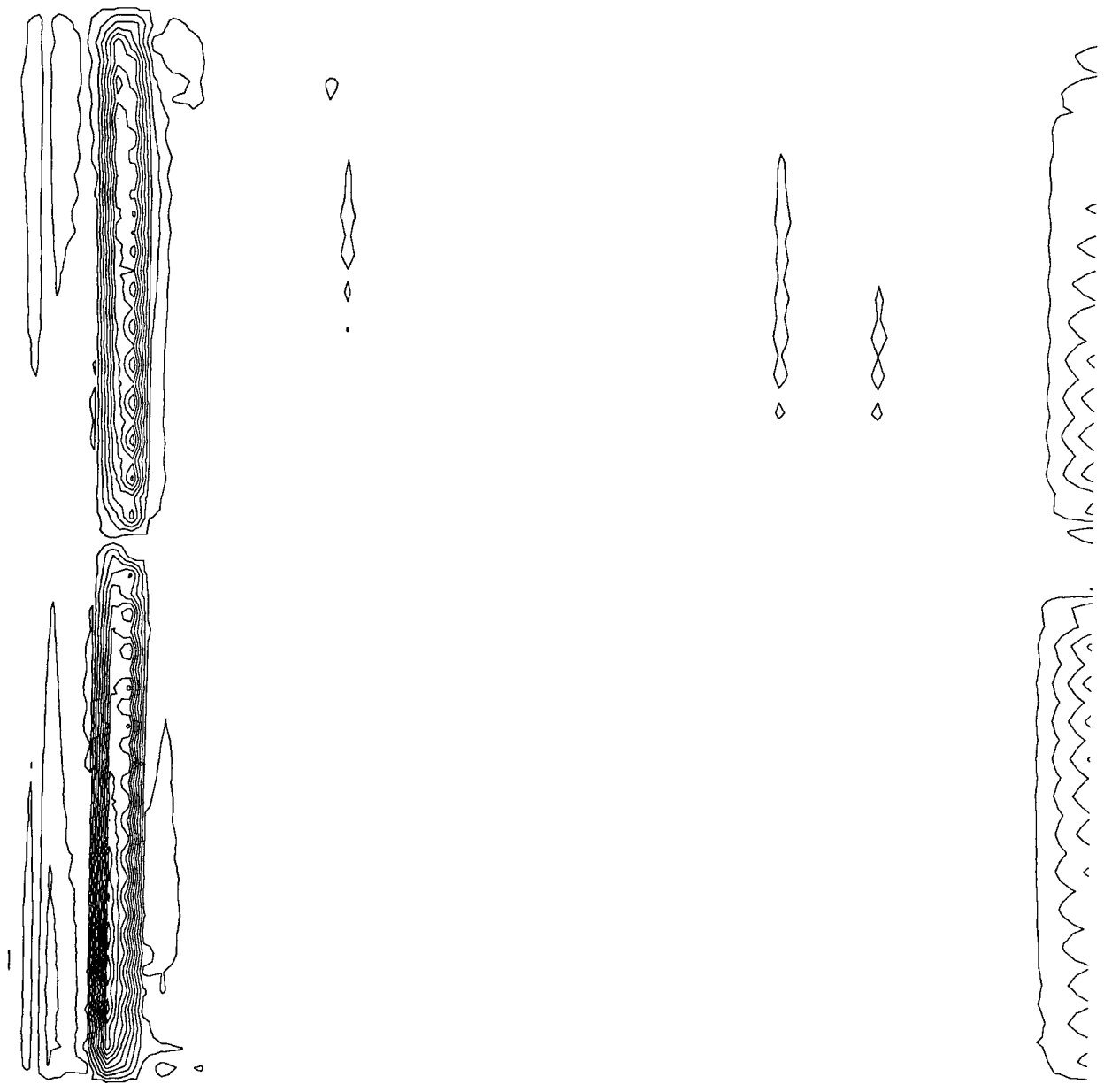

v Velocity Contour

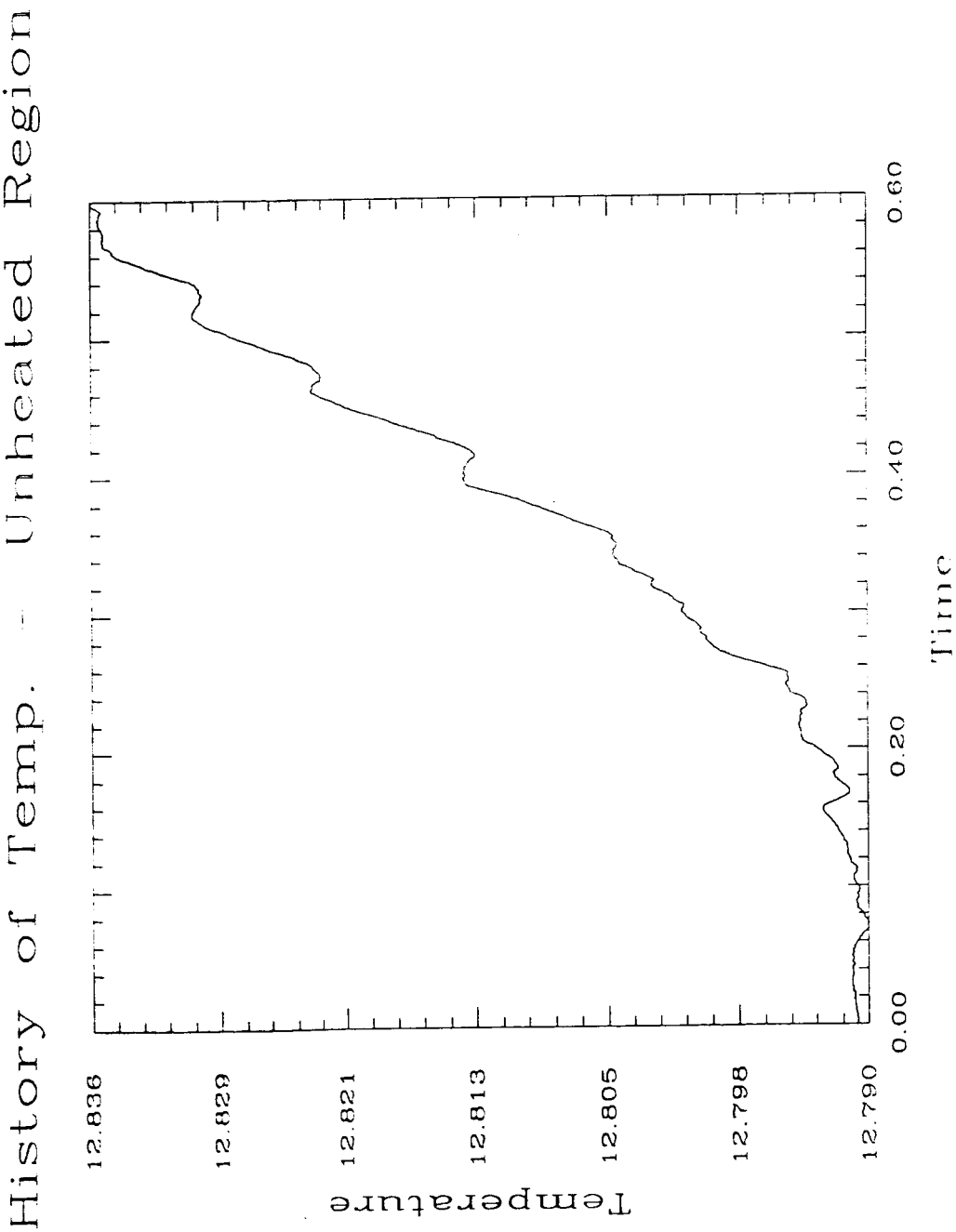
History of Temp. - Unheated Region
Temperature
12.836
12.829
12.821
12.813
12.805
12.798
12.790
0.00
0.20
0.40
0.60
Time

Figure 8

Figure 9

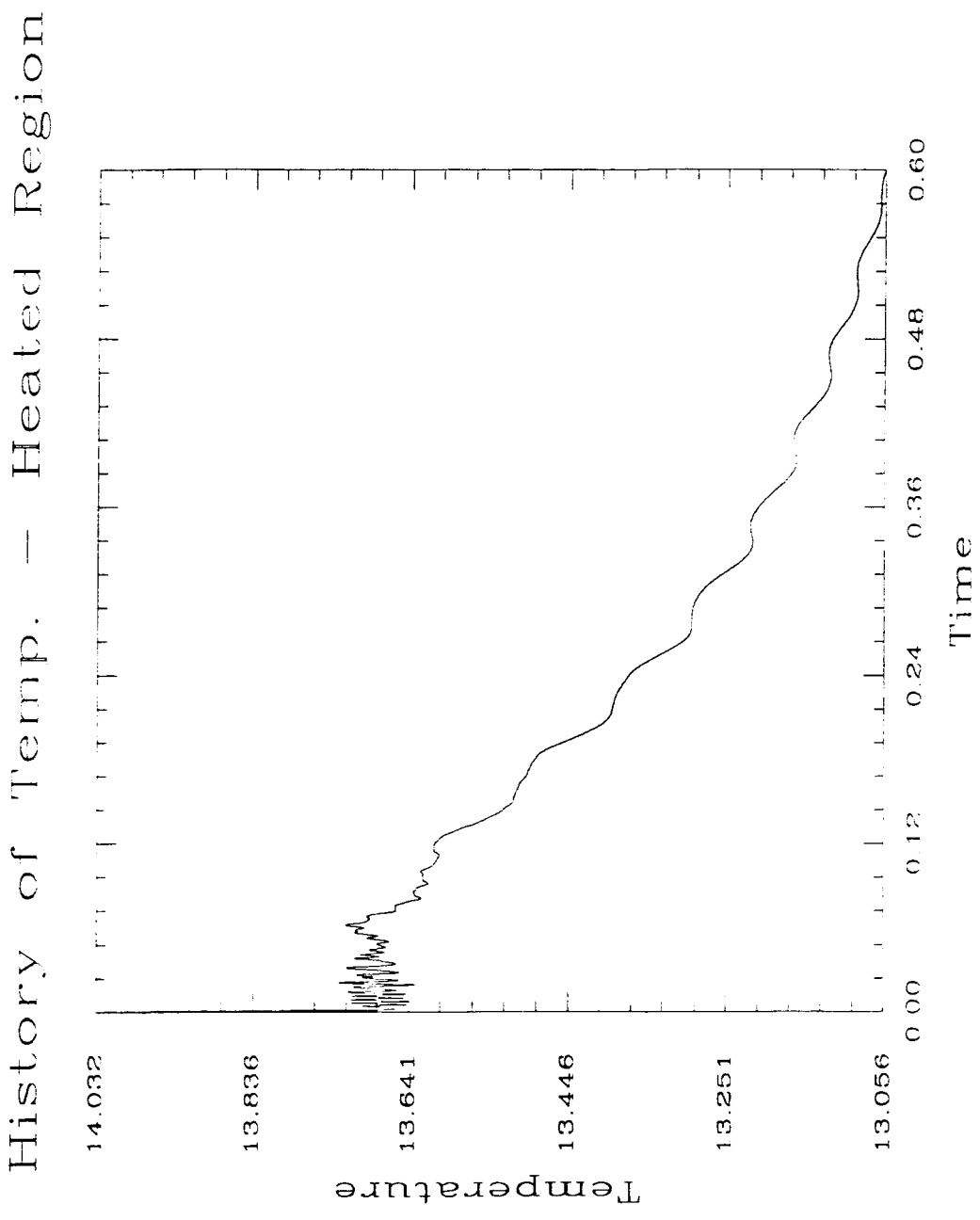
History of Temp. — Heated Region
Temperature
14.032
13.836
13.641
13.446
13.251
13.056
0.00
0.12
0.24
0.36
0.48
0.60
Time

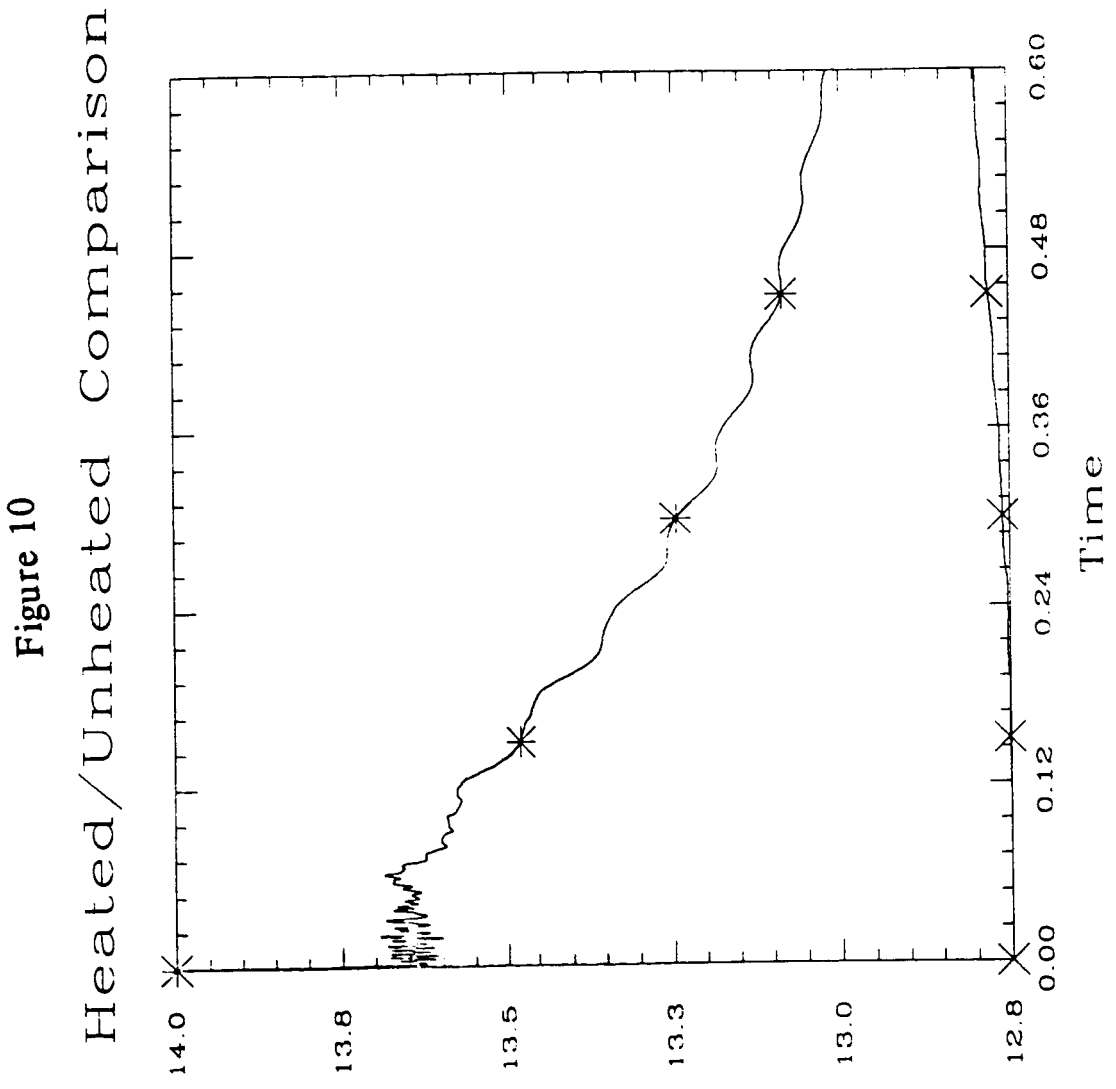
Heated/Unheated Comparison
14.0
13.8
13.5
13.3
13.0
12.8
0.00
0.12
0.24
0.36
0.48
0.60
Time

Figure 10

References

[1] Abarbanal, S., Bayliss, A., and Lustman, L.L., "Non-Reflecting Boundary Conditions for the Compressible Navier-Stokes Equations," NASA CR 178076 (1986).

[2] Bayliss, A. Parikh, P., Maestrello, L. and Turkel, E., "A Fourth Order Scheme for The Unsteady Compressible Navier-Stokes Equations," AIAA Paper 85-1694 (1985)

[3] Gottelib, D. and Turkel, E., "Dissipative Two-Four Methods for Time-Dependent Problems," Math. Comp. 30 (1976), pp. 703-723.

[4] Harris, J.E., "Numerical Solution of The Equations for Compressible Laminar, Transitional and Turbulent Boundary Layers and Comparison with Experimental Data," NASA TR-R-368 (1971).

[5] Rudy, D. and Strikwerda, J.C., "A Non-Reflecting Boundary Condition for Subsonic Navier-Stokes Calculations," J. Comp. Phys., 36, (1980), 55-70.

[6] Rudy, D. and Strikwerda, J.C., "Boundary Conditions for Subsonic Compressible Navier-Stokes Calculations," Computers and Fluids, 9, (1981), 327-328

[7] Spradley, L.W. and Churchill, S.W., "Pressure and Boundary Driven Thermal Convection In a Rectangular Enclosure," J. Fluid. Mech., Vol. 70, Part 4, (1975), pp. 705-720.

[8] Hedström, G.W., "Non-Reflecting Boundary Conditions for Nonlinear Hyperbolic Systems," J. Comp. Phys., Vol. 20, 1979, pp. 222-237.

[9] Anderson, D.A., Tannehill, J.C., and Fletcher, R.H., "Computational Fluid Mechanics and Heat Transfer," McGraw-Hill, 1984.

[10] Roberts, G.O., "Computational Methods for Boundary Layer Problems," Proc. 2nd Int. Conf. Numer. Meth. in Fluid Dynamics, Lecture Notes in Physics 8, Springer-Verlag, NY, (1971).

Standard Bibliographic Page

1. Report No. NASA CR-178333 ICASE Report No. 87-42	2. Government Accession No.	3. Recipient's Catalog No.
4. Title and Subtitle COMPRESSIBLE NAVIER-STOKES EQUATIONS: A STUDY OF LEADING EDGE EFFECTS		5. Report Date July 1987 6. Performing Organization Code
7. Author(s) S. I. Hariharan and P. R. Karbhari		8. Performing Organization Report No. 87-42
9. Performing Organization Name and Address Institute for Computer Applications in Science and Engineering Mail Stop 132C, NASA Langley Research Center Hampton, VA 23665-5225		10. Work Unit No. 505-90-21-01 11. Contract or Grant No. NAS1-18107
12. Sponsoring Agency Name and Address National Aeronautics and Space Administration Washington, D.C. 20546		13. Type of Report and Period Covered Contractor Report 14. Sponsoring Agency Code
15. Supplementary Notes Langley Technical Monitor: J. C. South Final Report		Submitted to J. Comput. Phys.

16. Abstract

In this study, we have developed a computational method that allows numerical calculations of the time dependent compressible Navier-Stokes equations. The current results concern a study of flow past a semi-infinite flat plate. Flow develops from given inflow conditions upstream and passes over the flat plate to leave the computational domain without reflecting at the downstream boundary. Leading edge effects are included in this paper. In addition, specification of a heated region which gets convected with the flow is considered. The time history of this convection is obtained, and it exhibits a wave phenomena.

17. Key Words (Suggested by Authors(s))	18. Distribution Statement
Navier-Stokes equations, compressibility, leading edge, finite differences	34 - Fluid Mechanics and Heat Transfer 64 - Numerical Analysis Unclassified - unlimited

19. Security Classif.(of this report)	20. Security Classif.(of this page)	21. No. of Pages	22. Price
Unclassified	Unclassified	26	A03

For sale by the National Technical Information Service, Springfield, Virginia 22161

NASA-Langley, 1987